This paper is available on line at http://www.mcponline.org

Down-regulation of Ras-related Protein Rab 5C-dependent Endocytosis and Glycolysis in Cisplatin-resistant Ovarian Cancer Cell Lines*[S]

Lixu Jin§, Yi Huo‡**, Zhiguo Zheng¶, Xiaoyong Jiang‡, Haiyun Deng§, Yuling Chen‡, Qingquan Lian§, Renshan Ge§, and Haiteng Deng‡‖**

Drug resistance poses a major challenge to ovarian cancer treatment. Understanding mechanisms of drug resistance is important for finding new therapeutic targets. In the present work, a cisplatin-resistant ovarian cancer cell line A2780-DR was established with a resistance index of 6.64. The cellular accumulation of cisplatin was significantly reduced in A2780-DR cells as compared with A2780 cells consistent with the general character of drug resistance. Quantitative proteomic analysis identified 340 differentially expressed proteins between A2780 and A2780-DR cells, which involve in diverse cellular processes, including metabolic process, cellular component biogenesis, cellular processes, and stress responses. Expression levels of Ras-related proteins Rab 5C and Rab 11B in A2780-DR cells were lower than those in A2780 cells as confirmed by real-time quantitative PCR and Western blotting. The short hairpin (sh)RNA-mediated knockdown of Rab 5C in A2780 cells resulted in markedly increased resistance to cisplatin whereas overexpression of Rab 5C in A2780-DR cells increases sensitivity to cisplatin, demonstrating that Rab 5C-dependent endocytosis plays an important role in cisplatin resistance. Our results also showed that expressions of glycolytic enzymes pyruvate kinase, glucose-6-phosphate isomerase, fructose-bisphosphate aldolase, lactate dehydrogenase, and phosphoglycerate kinase 1 were down-regulated in drug resistant cells, indicating drug resistance in ovarian cancer is directly associated with a decrease in glycolysis. Furthermore, it was found that glutathione reductase were up-regulated in A2780-DR, whereas vimentin, HSP90, and Annexin A1 and A2 were down-regulated. Taken together, our results suggest that drug resistance in ovarian cancer cell line A2780 is caused by multifactorial traits, including the down-regulation of Rab 5C-dependent endocytosis of cisplatin, glycolytic enzymes, and vimentin, and up-regulation of antioxidant proteins, suggesting Rab 5C is a potential target for treatment of drug-resistant ovarian cancer. This constitutes a further step toward a comprehensive understanding of drug resistance in ovarian cancer. ***Molecular & Cellular Proteomics 13: 10.1074/mcp.M113.033217, 3138–3151, 2014.***

Ovarian cancer is the major cause of death in women with gynecological cancer. Early diagnosis of ovarian cancer is difficult, while its progression is fast. The standard treatment is surgical removal followed by platinum-taxane chemotherapy. However, the efficacy of the traditional surgery and chemotherapy is rather compromised and platinum resistant cancer recurs in ~25% of patients within six months, and the overall five-year survival rate is about 31% (1–3). Virtually no efficient second line treatment is available. In order to increase survival rates from ovarian cancer and enhance patients' quality of life, new therapeutic targets are urgently required, necessitating a deeper understanding of molecular mechanisms of drug resistance.

Mechanisms of drug-resistance in ovarian cancer have been extensively studied over the last 30 years. Earlier studies have found that multiple factors are linked to drug resistance in human ovarian cancer including reduced intracellular drug accumulation, intracellular cisplatin inactivation, and increased DNA repair (4). Reduced cellular drug accumulation is mediated by the copper transporter-1 responsible for the influx of cisplatin (5–9) and MDR1, which encodes an integral membrane protein named P-glycoprotein for the active efflux of platinum drugs. Up-regulation of MDR1 has been observed in cisplatin-treated ovarian cancer cells although cisplatin is not a substrate of P-glycoprotein (10–13). A fraction of intracellular cisplatin can be converted into cisplatin-thiol conjugates by glutathione-S-transferase (GST) π, leading to inactivation of cisplatin. Up-regulation of both GSTπ and γ-glutamylcysteine synthetase has been associated with cisplatin resistance in ovarian, cervical and lung cancer cell lines (14–18). Binding of cisplatin to DNA leads to intrastrand or interstrand cross-links that alter the structure of the DNA molecule causing DNA damage. It has been amply documented that pathways for recognition and repair of damaged

From the ‡School of Life Sciences, Tsinghua University, Beijing, China; §The Second Affiliated Hospital of Wenzhou Medical University, Wenzhou, China; ¶Zhejiang Tumor Hospital, Hangzhou, China.

Received, August 6, 2013 and in revised form, July 28, 2014

Published, MCP Papers in Press, August 5, 2014, DOI 10.1074/mcp.M113.033217

Author contributions: Q.L., R.G., and Haiteng Deng designed research; L.J., Y.H., Z.Z., X.J., and Haiyun Deng performed research; L.J., Y.H., Z.Z., Y.C., and Haiteng Deng analyzed data; Haiteng Deng wrote the paper.

DNA are up-regulated in drug-resistant cancer cells (19–26). Furthermore, the secondary mutations have been identified, which restore the wild-type BRCA2 reading frame enhancing the acquired resistance to platinum-based chemotherapy (24). Alternations in other signaling pathways have also been found in drug resistant ovarian cancer (27–29). For example, DNA-PK phosphorylates RAC-alpha serine/threonine-protein kinase (AKT) and inhibits cisplatin-mediated apoptosis (28); and silencing of HDAC4 increases acetyl-STAT1 levels to prevent platinum-induced STAT1 activation and restore cisplatin sensitivity (29).

Proteomics is playing an increasingly important role in identifying differentially expressed proteins between drug-resistant and drug sensitive ovarian cancer cells (30–35). An earlier study has identified 57 differentially expressed proteins in human ovarian cancer cells and their platinum-resistant sublines, including annexin A3, destrin, cofilin 1, Glutathione-S-transferase omega 1, and cytosolic NADP+-dependent isocitrate dehydrogenase using 2D gel electrophoresis (30). Employing a similar 2D gel electrophoresis approach, changes in protein expressions of capsid glycoprotein, fructose-bisphosphate aldolase C, heterogeneous nuclear ribonucleoproteins A2/B1, putative RNA-binding protein 3, Ran-specific GTPase-activating protein, ubiquitin carboxyl-terminal hydrolase isozyme L1, stathmin, ATPSH protein, chromobox protein homolog3, and phosphoglycerate kinase 1 (PGK)[1] were found in A2780 and drug-resistant A2780 cells (32). It is worth mentioning that ALDO and PGK are glycolytic enzymes, indicating that glycolysis plays a role in drug resistance. Studies have demonstrated that resistance to platinum drugs in ovarian cancer cells is linked to mitochondrial dysfunctions in oxidative phosphorylation and energy production (36–40). Mitochondrial proteomic analysis of drug-resistant cells has shown that five mitochondrial proteins (ATP-a, PRDX3, PHB, ETF, and ALDH) that participate in the electron transport respiratory chain are down-regulated in drug-resistant cell lines (41). PRDX3 is involved in redox regulation of the cell to protect radical-sensitive enzymes from oxidative damage. However, it is not clear how down-regulation of PRDX3 is associated with drug-resistance. A more recent study showed that activated leukocyte cell adhesion molecule (ALCA) and A kinase anchoring protein 12 (AKAP12) are elevated in drug-resistant A2780-CP20 cells by quantifying the mitochondrial proteins (42). Despite these efforts, the drug-resistance mechanisms are not yet well understood.

In this work, we established and characterized a drug-resistant cell line A2780-DR from A2780 cells. We employed a quantitative proteomic method to identify the differentially expressed proteins between A2780 and A2780-DR cells. Expression changes of selected proteins were confirmed by qPCR and Western blotting. We also used shRNA silencing to explore functions of Rab 5C and Rab 11B proteins in drug resistance. Our data indicate that the differentially expressed proteins participate in a variety of cellular processes and enhance our understanding of the mechanisms of drug resistance in ovarian cancer cells.

[1] The abbreviations used are: PGP, phosphoglycerate kinase; ROS, reactive oxygen species; GO, Gene Ontology; PKM, pyruvate kinase.

MATERIALS AND METHODS

Chemicals and Reagents—Dulbecco's Modified Eagle Medium (DMEM), fetal bovine serum, and penicillin-streptomycin were purchased from Wistent (Saint-Jean-Baptiste, CA). Dithiothreitol (DTT) was purchased from Calbiochem (San Diego, CA). The A2780 cell line was obtained from the Tumor Cell Bank of the Chinese Academy of Medical Sciences (Beijing, China). Sequencing grade modified trypsin was purchased from Promega (Fitchburg, WI). The propidium iodide staining kit was purchased from Solarbio (Beijing, China). The TMT labeling kit was purchased from Thermo-Pierce Biotechnology (Rockford, IL).

Cell Culture and Establishment of Cisplatin Resistant Subline—The human epithelial ovarian cancer cell line A2780 cells were maintained in DMEM media supplemented with 10% fetal bovine serum and penicillin (100 U/ml)–streptomycin (100 mg/ml) at 37 °C with 5% CO_2. Cells were grown as monolayer cultures in 10 cm tissue culture plate and passaged when they had reached about 90% confluence. A monoclonal strain was separated by flow cytometry and further cultured to obtain A2780 cisplatin resistant strain (A2780-DR) by incubation with stepwise increasing cisplatin concentrations. Backups of all cells were stored with 10% DMSO. Every 20 passages, a new backup of cells was thawed to ascertain that resistance mechanisms were unchanged during long term cultivation. The relative cisplatin resistance was determined by cell viability assay.

Cell Cytotoxicity Assay—Effects of cisplatin on cell proliferation in A2780 and A2780-DR were analyzed with the Cell Counting Kit-8 (CCK-8) from Dojindo (Japan). A2780 and A2780-DR cells (8×10^3 each) were seeded into wells in 96-well cell culture microplates and incubated for 16 h prior to cisplatin treatment. Cells were then treated with cisplatin at different concentrations (0, 20, 40, 80, 160, and 320 μM) in triplicates for 24 h. The CCK8 reagent was added to treated cells and incubated at 37 °C for 2 h. Optical density (OD) was measured at 450 nm with a microplate reader (Bio-Rad, Hercules). Cell viability was calculated as the percentage of variable cells compared with untreated cells. The experiment was repeated three times and the IC50 was calculated by SPSS13.0 (SPSS Inc., Chicago, IL,). The lower the IC50 value, the higher the potency against cell proliferation.

Sample Preparation and Quantitative Proteomic Analysis—About 6×10^5 cells were lysed using RIPA lysis buffer (Solabio, Beijing, China), and protein concentrations were measured using the BCA method. Equal amount of proteins from untreated- and treated-samples (about 30 μg) were separated by 1D SDS-PAGE, respectively. The gel bands of interest were excised from the gel, reduced with 25 mM of dithiotreitol, and alkylated with 55 mM iodoacetamide. In gel digestion was then carried out with sequencing grade modified trypsin in 50 mM ammonium bicarbonate at 37 °C overnight. The peptides were extracted twice with 0.1% trifluoroacetic acid in 50% acetonitrile aqueous solution for 30 min. Extracts were then centrifuged in a speedvac to reduce the volume. Tryptic peptides were redissolved in 50 μl 200 mM Tetraethylammonium Bromide (TEAB), and 2 μl TMTsixplex labeling reagent was added to each sample according to the manufacture's instruction. The reaction was incubated for 1 h at room temperature. Then, 0.5 μl of 5% hydroxylamine (pH 9–10) was added to the reaction mixture and incubated for 15 min to quench the reaction. Equal amount of proteins from A2780 and A2780-DR cells were combined and analyzed by LC-MS/MS.

For LC-MS/MS analysis, the TMT-labeled peptides were separated by a 65 min gradient elution at a flow rate 0.250 μl/min with a Thermo-Dionex Ultimate 3000 HPLC system, which was directly interfaced with a Thermo Scientific Q Exactive mass spectrometer. The analytical column was a home-made fused silica capillary column (75 μm ID, 150 mm length; Upchurch, Oak Harbor, WA) packed with C-18 resin (300 Å, 5 μm, Varian, Lexington, MA). Mobile phase A consisted of 0.1% formic acid, and mobile phase B consisted of 100% acetonitrile and 0.1% formic acid. The Q Exactive mass spectrometer was operated in the data-dependent acquisition mode using Xcalibur 2.1.2 software and there was a single full-scan mass spectrum in the orbitrap (400–1800 *m/z*, 60,000 resolution) followed by 10 data-dependent MS/MS scans at 27% normalized collision energy.

The MS/MS spectra from each LC-MS/MS run were searched against the human.fasta from UniProt (release date of March 19, 2014; 68406 entries) using an in-house Proteome Discoverer (Version PD1.4, Thermo-Fisher Scientific). The search criteria were as follows: full tryptic specificity was required; one missed cleavage was allowed; carbamidomethylation (C) and TMT sixplex (K and N-terminal) were set as the fixed modifications; the oxidation (M) was set as the variable modification; precursor ion mass tolerances were set at 10 ppm for all MS acquired in an orbitrap mass analyzer; and the fragment ion mass tolerance was set at 20 mmu for all MS2 spectra acquired. The peptide false discovery rate was calculated using Percolator provided by PD. When the q value was smaller than 1%, the peptide spectrum match was considered to be correct. False discovery was determined based on peptide spectrum match when searched against the reverse, decoy database. Peptides only assigned to a given protein group were considered as unique. The false discovery rate was also set to 0.01 for protein identifications. Relative protein quantification was performed using Proteome Discoverer software (Version 1.4) according to manufacturer's instructions on the six reporter ion intensities per peptide. Quantitation was carried out only for proteins with two or more unique peptide matches. Protein ratios were calculated as the median of all peptide hits belonging to a protein. Quantitative precision was expressed as protein ratio variability. Differentially expressed proteins were further confirmed by qPCR or Western blotting. The mass spectrometry proteomics data have been deposited to the ProteomeXchange Consortium via the PRIDE partner repository with the data set identifier PXD001176.

Real-time Quantitative PCR (qPCR)—Cells were harvested 48 h after transfection. Total RNA was extracted by the SV Total RNA Isolation System. cDNA was synthesized from 0.8 μg total RNA using the GoScript™ Reverse Transcription System. All qPCR was performed using the Roche LightCycler® 480II Detection System with SYBR green incorporation according to the manufacturer's instructions. The primers were either designed by using the Primer Premier 5 software or from Primer Bank (http://pga.mgh.harvard.edu primerbank/). To prevent amplification of genomic DNA, all target primers span exon-exon junctions. The specific PCR products were confirmed by melting curve analysis. Relative expression was analyzed using the $2^{-\Delta\Delta Ct}$ method. Primer sequences for qPCR are listed in supplemental Table S1.

Western Blotting—Cells were harvested and lysed in RIPA lysis buffer. For shRNA transfected cells, cells were lysed at 72 h after transfection. The supernatants were collected after centrifugation at 14,000 × *g* for 10 min at 4 °C. Protein concentrations were determined using the BCA protein assay kit. Proteins were separated on a 12% SDS-PAGE gel and transferred onto a polyvinyl diflouride transfer membrane by electroblotting. After blocking with 5% nonfat milk for 2 h at room temperature, the membrane was incubated overnight at 4 °C with 1000× diluted primary antibody, washed with Phosphate Buffered Saline with Tween 20 (PBST) buffer for three times, then incubated with 1000× diluted anti-mouse or anti-rabbit secondary antibody labeled with horseradish peroxidase at room temperature for 2 h. The membrane was further washed with PBST buffer three times and developed using ECL reagents (Engreen, China). β-actin was detected with anti-β-actin antibody as an internal control. BioRad Image Lab software was used to analyze the images.

Determination of Cellular Platinum Accumulation—The cellular platinum accumulation was determined by the method described by Kayoko Minakata (43). Briefly, equal amount of A2780 and A2780-DR cells (about 4×10^6) were collected after 10 μM cisplatin treatment for 24 h. Cell pellets were washed three times with ice-cold PBS. Cell pellet was wet-ashed in 30 μl concentrated HNO_3 at 85 °C for 8 h. The pH of wet-ashed solution was adjusted to 3–7 with either 10 M NaOH or 7 M HNO_3. 30 μl of 1 M Diethyldithiocarbamate (DDC) was then added to the solution, in which DDC forms a complex with Pt by replacing other bonded ligands. After 3 min, 30 μl of isoamylalcohol was added and mixed for 30 s, and separated by centrifugation. The isoamylalcohol layer was mixed with 30 μl of 1 M oxalic acid for 10 s and centrifuged. A 1 μl aliquot of the isoamylalcohol layer was subjected to electrospray ionization mass spectrometry. Measurements were done in triplicate to determine standard errors of the mean (shown as error bars).

Short Hairpin RNA (ShRNA)-mediated Gene Silencing—The shRNAs against Rab 5C and Rab 11B were designed by the Invitrogen RNAi design tool (http://www.invitrogen.com) and synthesized by Invitrogen, LTD. Nontargeting negative control of shRNA (NCi) was also synthesized. The shRNA sequences are displayed in supplemental Table S2. The oligonucleotides were annealed and inserted into the pll3.7 siRNA expression vector to generate shRNA. The A2780 cells were plated the day before transfection and allowed to grow to 70–80% confluence. The cells were transiently transfected with Rab 5C-shRNA-pll3.7 or Rab 11B-shRNA-pll3.7 respectively with polyethylenimine (PEI) in DMEM. The effectiveness of shRNA in inhibiting Rab 5C and Rab 11B expression was evaluated by real time RT-PCR (48 h after the transfection) and Western blotting analysis (72 h after the transfection). Cells transfected with the plasmid NCi-pll3.7 served as the control.

Overexpression of Rab 5C in A2780-DR Cells—The gene of Rab 5C was cloned from the mRNA by RT-PCR from the Raji cell line, which was then subcloned into eukaryotic plasmid pcDNA3.1B (Invitrogen). The primer sequences are displayed in supplemental Table S2. Briefly, A2780-DR cells were plated the day before transfection and allowed to grow to 70–80% confluence. The cells were transiently transfected with pcDNA3.1 and Rab 5C-pcDNA3.1, respectively. The expression of Rab 5C was examined by Western blotting after 72 h transfection.

Detection of Reactive Oxygen Species (ROS) in A2780 and A2780-DR Cells—The ROS in untreated and azacytidine-treated cells was detected using the Image-iT™ LIVE Green Reactive Oxygen Species Detection Kit (Molecular Probes, Inc. Eugene, OR) following manufacturer's instructions. Briefly, A2780 and A2780-DR cells (2.5 × 105 each) were plated in triplicates in six-well plate the day before the test. After 48 h growth, the cells were collected by centrifugation and washed once with warm HBSS/Ca/Mg. Cells were resuspended with 500 μl of the 25 μM carboxy-H2DCFDA working solution for 25 min at 37 °C, followed by addition of the Hoechst 33342 reagent to the reaction mixture at the final concentration of 1.0 μM and incubation for 5 min. The final products were gently washed with 1 ml HBSS/Ca/Mg immediately followed by imaging with Zeiss 710 Confocal Microscopy.

RESULTS

Characterization of the Drug-resistant A2780 Cell Line—The drug-resistant cell line A2780-DR was established by the stepwise selection of A2780 cells cultured in growth media

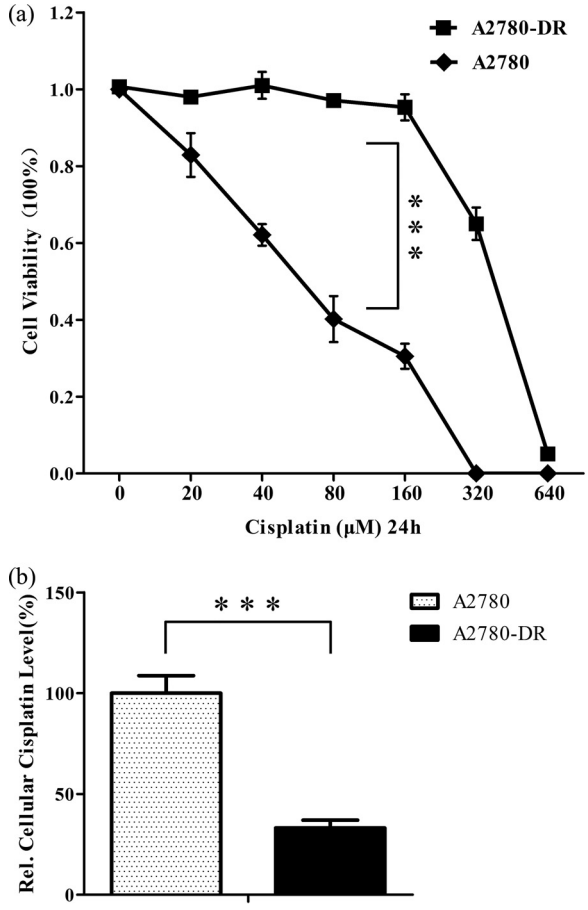

FIG. 1. ***A*, Cell cytotoxicity assays.** Percentage of viable A2780-DR and A2780 cells treated with cisplatin at different concentrations for 24 h determined by using CCK-8 assay. Results are expressed as the mean of three experiments with p value <0.001; *B*, accumulation of cisplatin in 10 μM cisplatin treated A2780 and A2780-DR cells for 24 h as determined by electrospray ionization mass spectrometry. *** $p <$ 0.001.

TABLE I
IC50 and Resistance Index of A2780-related cells to cisplatin treatment

	IC50 (μM)	RI
A2780	61.0 ± 2.3	1
A2780-DR	404.9 ± 15.1	6.6
EV-A2780[a]	54.6 ± 5.0	1
ShRNA(Rab5C)-A2780	103.3 ± 6.2	1.9
EV-A2780	45.1 ± 2.7	1
ShRNA(Rab11B)-A2780	62.7 ± 3.2	1.4

[a] Empty vector transfected cells.

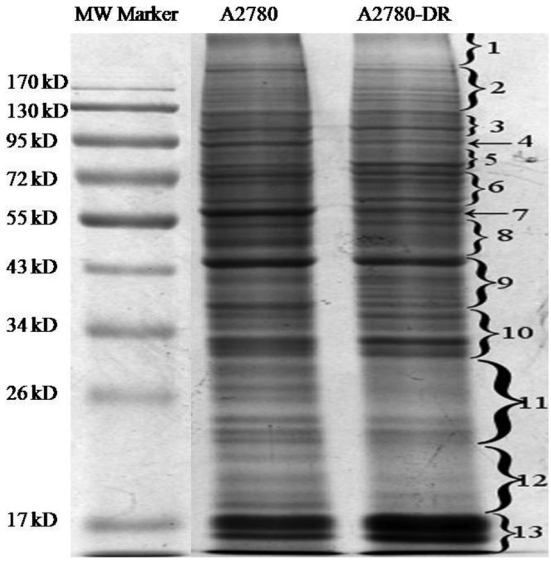

FIG. 2. **1D SDS-PAGE gel image of A2780 and A2780-DR cells.** Lane 1, molecular weight markers; Lane 2, proteins from A2780 cells; Lane 3, proteins from A2780-DR cells; and bands excised from the gel with differentially expressed proteins are labeled with numeric numbers.

with increasing drug concentrations over a period of 6 months. To determine the sensitivity of A2780 and A2780-DR cells to cisplatin, cells were treated with different concentrations of cisplatin for 24 h and cell viability was measured by the Cell Counting Kit-8 (CCK-8) assay that allows sensitive colorimetric determination of cell viability and drug-sensitivity. The dose-dependent effects of cisplatin were represented as the percentage of viable cells as compared with untreated cells (Fig. 1*A*). When cells were treated with 80 μM cisplatin for 24h, percentages of viable cells were 40 and 100% for A2780 and A2780-DR cells, respectively. The inhibitory concentration 50% (IC50) and resistance index (RI) values of the two cell lines are displayed in Table I, indicating that A2780-DR is cisplatin resistant. The resistant phenotype is stable as the values of IC50 and RI have no significant changes over a period of 4 months in drug-free medium.

We also analyzed the total cellular Pt accumulation in sensitive and resistant cells following exposure to 10 μM cisplatin treatment for 24 h. The relative cisplatin concentrations were displayed in Fig. 1*B* as determined by mass spectrometry. After treatment with cisplatin, total intracellular Pt in A2780-DR is about one third of that in the parent cell line A2780, indicating significant reduction of cisplatin accumulation in drug-resistant cells.

Proteomic Analysis of A2780 and A2780-DR Cells—Next, proteomic analysis was carried out on A2780 and A2780-DR cells. Equal amounts of proteins from A2780 and A2780-DR cells were loaded and separated by 1D SDS-PAGE (Fig. 2). Differentially expressed proteins were identified and quantified using TMT-labeling. The experiments were repeated three times and ~1900 proteins were identified for each cell line. The false-positive rate was set to be less than 1%. Based on TMT ratios (>2.0 or <0.6) in proteins that have two or more unique peptides, 340 proteins were found to be differentially expressed between A2780 and A2780-DR cells, of which 268 proteins are down-regulated and 72 up-regulated (Table II and III). The major protein in band 7 that was down-regulated in A2780-DR was identified as vimentin. HSP90α and HSP90β in

TABLE II
Up-regulated proteins in cisplatin resistant cells

Accession	Description	Score	Coverage (%)	Unique peptides	A2780-DR/A2780
E9PM69	26S protease regulatory subunit 6A	17	15	5	3.5
O00231	26S proteasome non-ATPase regulatory subunit 11	18	16	6	5.1
P36578	60S ribosomal protein L4	77	30	12	5.1
B4DQJ8	6-phosphogluconate dehydrogenase, decarboxylating	23	24	8	3.7
G3V4F2	Acyl-coenzyme A thioesterase 1	14	14	4	3.6
P30520	Adenylosuccinatesynthetaseisozyme 2	16	13	4	4.4
P30837	Aldehyde dehydrogenase X, mitochondrial	22	18	6	6.3
F8VS02	Alpha-aminoadipicsemialdehyde dehydrogenase	17	17	7	6.2
P06733	Alpha-enolase	217	53	16	4.8
B4DT77	Annexin	23	12	4	2.4
P25705	ATP synthase subunit alpha, mitochondrial	136	45	19	6.8
P06576	ATP synthase subunit beta, mitochondrial	199	52	20	5.4
R4GMX5	Basigin (Fragment)	11	36	3	4.7
H3BS10	Beta-hexosaminidase	17	8	3	2.3
Q13895	Bystin	10	6	3	4.2
P10644	cAMP-dependent protein kinase type I-alpha regulatory subunit	13	18	6	3.4
C9JP16	Cartilage-associated protein	12	12	5	5.3
P31930	Cytochrome b-c1 complex subunit 1, mitochondrial	27	17	6	5.7
B7Z5W8	Dihydrolipoyllysine-residue succinyltransferase component	11	11	4	6.4
P39656	Dolichyl-diphosphooligosaccharide–protein glycosyltransferase 48 kDa subunit	46	21	9	5.5
Q05639	Elongation factor 1-alpha 2	256	20	2	3.1
P26641	Elongation factor 1-gamma	62	32	13	4.7
P49411	Elongation factor Tu, mitochondrial	88	27	11	4.5
F5H0C8	Enolase	52	11	2	4.1
P07099	Epoxide hydrolase 1	42	24	11	5.3
Q96CG1	ETF1 protein	13	6	2	2.7
P38919	Eukaryotic initiation factor 4A-III	31	21	6	4.7
H7BZU1	Eukaryotic translation initiation factor 2 subunit 3 (Fragment)	10	11	2	3.9
O00303	Eukaryotic translation initiation factor 3 subunit F	17	17	5	3.6
J3KNT0	Fascin	18	23	9	4.1
J3QRD1	Fatty aldehyde dehydrogenase	27	14	5	8.1
P39748	Flap endonuclease 1	12	8	3	4.6
P00367	Glutamate dehydrogenase 1, mitochondrial	22	18	8	5.9
P52597	Heterogeneous nuclear ribonucleoprotein F	47	14	2	3.6
P31943	Heterogeneous nuclear ribonucleoprotein H	94	33	5	4.5
P55795	Heterogeneous nuclear ribonucleoprotein H2	51	18	2	4.3
B3KWE1	Histidine–tRNA ligase, cytoplasmic	15	6	3	3.9
P0C0S5	Histone H2A.Z	283	31	2	2.1
H7C3I1	Hsc70-interacting protein (Fragment)	17	23	3	6.6
Q6YN16	Hydroxysteroid dehydrogenase-like protein 2	12	8	3	8.6
P43686-2	Isoform 2 of 26S protease regulatory subunit 6B	15	19	6	6.0
P62195-2	Isoform 2 of 26S protease regulatory subunit 8	15	12	3	3.5
Q16401-2	Isoform 2 of 26S proteasome non-ATPase regulatory subunit 5	35	21	8	4.1
P28838-2	Isoform 2 of Cytosol aminopeptidase	26	19	8	6.9
Q9H0S4-2	Isoform 2 of Probable ATP-dependent RNA helicase DDX47	12	10	3	7.3
P35659-2	Isoform 2 of Protein DEK	17	11	4	4.3
P50395-2	Isoform 2 of Rab GDP dissociation inhibitor beta	33	26	5	4.9
Q8NBS9-2	Isoform 2 of Thioredoxin domain-containing protein 5	47	39	11	4.3
O14773-2	Isoform 2 of Tripeptidyl-peptidase 1	10	9	2	4.9
P34897-3	Isoform 3 of Serine hydroxymethyltransferase, mitochondrial	37	20	9	6.5
P00390-5	Isoform 4 of Glutathione reductase, mitochondrial	25	11	4	6.1
O60664-4	Isoform 4 of Perilipin-3	24	21	6	5.6
P07954-2	Isoform Cytoplasmic of Fumaratehydratase, mitochondrial	28	13	6	5.7
P05455	Lupus La protein	19	16	6	6.3
Q10713	Mitochondrial-processing peptidase subunit alpha	13	10	5	6.3
E7ERZ4	Mitochondrial-processing peptidase subunit beta	11	12	3	5.8
B4DEH8	Polyadenylate-binding protein 2	19	17	3	5.1
Q9UQ80	Proliferation-associated protein 2G4	23	18	7	3.3
B7Z254	Protein disulfide-isomerase A6	95	35	12	7.3
P49257	Protein ERGIC-53	17	7	3	4.8
P18754	Regulator of chromosome condensation	22	19	6	6.2
F8W914	Reticulon	12	12	3	3.6

TABLE II—*continued*

Accession	Description	Score	Coverage (%)	Unique peptides	A2780-DR/A2780
P00352	Retinal dehydrogenase 1	48	26	11	2.7
P13489	Ribonuclease inhibitor	15	17	5	4.2
Q9Y265	RuvB-like 1	67	31	10	4.6
Q9Y230	RuvB-like 2	36	21	8	3.7
O15269	Serine palmitoyltransferase 1	10	11	4	4.5
P50454	Serpin H1	171	52	19	4.0
Q13838	Spliceosome RNA helicase DDX39B	96	29	3	4.2
P55084	Trifunctional enzyme subunit beta, mitochondrial	21	24	10	7.0
P50552	Vasodilator-stimulated phosphoprotein	10	12	4	4.6
P04004	Vitronectin	11	5	2	2.7

band 4 were also down-regulated in the drug-resistant cells (Fig. 2). In order to understand the biological relevance of the identified proteins, Gene Ontology (GO) was used to categorize the differentially expressed proteins according to their molecular functions and biological processes. The annotations of gene lists are summarized via a pie plot using the PANTHER bioinformatics platform (http://www.pantherdb.org/) as shown in Fig. 3. Three hundred and thirty nine proteins were classified into several significant groups of biological processes including metabolic processes, cellular processes, cellular compartment organization, and apoptosis.

Verification of Differentially Expressed Proteins by Western blotting and qPCR—Among differentially expressed proteins (Table III), Ras-related protein Rab 5C and Rab 11B are down-regulated in the drug-resistant cells. Fig. 4 shows a ms/ms spectrum of a peptide ions that match to fragments of a tryptic peptide GVDLQENNPASR from Rab 5C and the insert shows fragments at the low mass range for the TMT-reporter ions, whose ratio indicates that the expression level of Rab 5C is three times higher in A2780 as compared with A2780-DR cells. Down-regulation of Rab 5C and Rab 11B was confirmed by Western blotting (Fig. 5*A*) and by qPCR analysis (Fig. 5*B*). Results from analysis of band intensities of Western blot are displayed in supplemental Table S3. Vimentin was the most abundant with the highest spectra count among the differentially expressed proteins and the down-regulation of vimentin was confirmed by Western blotting (Fig. 5*A*), showing that two bands at 54 and 56 kDa were barely visible for vimentin in A2780-DR cells. Western blotting also confirms that the expression level of PKM2 is down-regulated in A2780-DR cells (Fig. 5*A*). Proteomic analysis shows that a redox proteins glutathione reductase (GSR) is up-regulated in A2780-DR cells.

Rab 5C Mediated Cisplatin-resistance—To understand the role of Rab 5C and Rab 11B in drug-resistance, shRNAs were used to silence Rab 5C and Rab 11B in A2780 cells. The plasmid NCi-pll3.7 was also transfected into A2780 as the control to exclude effects of cytotoxicity caused by transfection. The silencing of Rab 5C and Rab 11B was verified by Western blotting and qPCR assays (supplemental Fig. S1). The expression level of Rab 5C mRNA decreased to 30% of that observed for NCi-pll3.7 -transfected cells, whereas the expression level of Rab 11B mRNA decreased to 57% of the control. The sensitivities of shRNA-transfected cells to cisplatin were analyzed by CCK8 assay after cells were treated with different concentrations of cisplatin for 24 h. When cells were treated with 40 μM cisplatin for 24 h, differences in sensitivity to cisplatin were observed among NCi-pll3.7- and Rab 5C shRNA-transfected cells. The change of drug resistance in Rab 11B shRNA-transfected cells is less significant as compared with A2780 cells. Results demonstrate that transfection of A2780 cells with shRNA against Rab 5C increases cell resistance to cisplatin. The IC50 and resistance index values of shRNA-transfected cell lines are 103.3 and 1.89 for Rab 5C, and 62.7 and 1.39 for Rab 11B (Table I).

To further explore Rab 5C mediated drug resistance, Rab 5C was sub-cloned into eukaryotic plasmid pcDNA3.1 that was transfected into A2780-DR cells. The overexpression of Rab 5C in A2780 cells was examined by Western blotting (supplemental Fig. S1*C*), showing that the expression level of Rab 5C in A2780-DR cells is three times higher than that in empty vector-transfected cells. The sensitivities of Rab 5C overexpressing cells to cisplatin were analyzed by CCK8 assay after cells were treated with different concentrations of cisplatin for 24 h (Fig. 6*C*), demonstrating that overexpression of Rab 5C in A2780-DR cells increases cell susceptibility to cisplatin.

DISCUSSION

Multidrug resistance is the main reason for the failure of ovarian cancer chemotherapy. The establishment of drug resistant cancer cell lines is an important step in providing an *in vitro* model for understanding the mechanism of drug resistance and for identifying new therapeutic targets. Cisplatin is a traditional anticancer drug used in clinical settings. In this study, we used human ovarian cell line A2780 as a model system to establish a cisplatin resistant cell line A2780-DR. By the stepwise increase of cisplatin concentration in the growth medium and selection of drug-resistance colonies for six months, we successfully established a cisplatin-resistant cell line with the resistance index 6.76. Using mass spectrometry analysis, it was found that Pt accumulation in A2780-DR cells

TABLE III
Down-regulated Proteins in cisplatin-resistant cells

Accession	Description	Score	Coverage (%)	Unique Peptides	A2780-DR/A2780
Q04917	14-3-3 protein eta	42	26	3	0.3
P61981	14-3-3 protein gamma	57	38	5	0.3
P27348	14-3-3 protein theta	55	27	2	0.3
P63104	14-3-3 protein zeta/delta	75	43	6	0.3
P62191	26S protease regulatory subunit 4	36	22	7	0.6
Q15008	26S proteasome non-ATPase regulatory subunit 6	31	11	4	0.3
R4GMR5	26S proteasome non-ATPase regulatory subunit 8	19	14	5	0.3
P82930	28S ribosomal protein S34, mitochondrial	12	22	5	0.5
P46783	40S ribosomal protein S10	24	23	3	0.3
P62277	40S ribosomal protein S13	22	38	5	0.5
P62269	40S ribosomal protein S18	21	24	4	0.6
P39019	40S ribosomal protein S19	34	48	9	0.6
P62851	40S ribosomal protein S25	26	21	3	0.4
F2Z2S8	40S ribosomal protein S3	15	33	4	0.6
P62701	40S ribosomal protein S4, X isoform	57	32	9	0.3
M0R0F0	40S ribosomal protein S5 (Fragment)	19	27	5	0.5
Q5JR95	40S ribosomal protein S8	21	38	6	0.2
P46781	40S ribosomal protein S9	19	18	4	0.5
C9J9K3	40S ribosomal protein SA (Fragment)	86	36	6	0.2
F8VU65	60S acidic ribosomal protein P0 (Fragment)	26	25	6	0.2
P62906	60S ribosomal protein L10a	20	24	6	0.3
P30050	60S ribosomal protein L12	13	23	3	0.5
P26373	60S ribosomal protein L13	28	27	6	0.3
E7EPB3	60S ribosomal protein L14	29	35	4	0.2
P61313	60S ribosomal protein L15	25	18	5	0.4
G3V203	60S ribosomal protein L18	17	25	4	0.5
P61353	60S ribosomal protein L27	15	21	3	0.6
E9PJD9	60S ribosomal protein L27a	15	34	3	0.5
P49207	60S ribosomal protein L34	18	21	3	0.5
Q02878	60S ribosomal protein L6	23	25	7	0.2
P18124	60S ribosomal protein L7	26	27	6	0.3
O95336	6-phosphogluconolactonase	11	14	3	0.4
P24752	Acetyl-CoA acetyltransferase, mitochondrial	30	22	8	0.4
H0YN26	Acidic leucine-rich nuclear phosphoprotein 32 family member A	15	18	2	0.3
O95433	Activator of 90 kDa heat shock protein ATPase homolog 1	19	18	5	0.3
Q01518	Adenylyl cyclase-associated protein 1	73	31	14	0.5
P12235	ADP/ATP translocase 1	128	32	2	0.3
P05141	ADP/ATP translocase 2	171	40	4	0.4
P61204	ADP-ribosylation factor 3	12	20	2	0.4
H0YN42	Annexin (Fragment)	28	33	8	0.4
P04083	Annexin A1	457	66	21	0.2
P02647	Apolipoprotein A-I	52	53	15	0.2
B7Z7E9	Aspartate aminotransferase	17	16	5	0.3
P00505	Aspartate aminotransferase, mitochondrial	48	18	8	0.5
P48047	ATP synthase subunit	11	27	4	0.5
O43681	ATPase ASNA1	11	7	3	0.4
Q08211	ATP-dependent RNA helicase A	346	34	36	0.5
Q92499	ATP-dependent RNA helicase DDX1	31	14	10	0.5
O95816	BAG family molecular chaperone regulator 2	21	27	6	0.4
P51572	B-cell receptor-associated protein 31	17	13	4	0.4
E9PK09	Bcl-2-associated transcription factor 1 (Fragment)	13	6	5	0.3
P07686	Beta-hexosaminidase subunit beta	30	13	6	0.4
P07814	Bifunctional glutamate/proline–tRNA ligase	39	12	17	0.4
P31327	Carbamoyl-phosphate synthase [ammonia], mitochondrial	22	8	9	0.4
E9PFZ2	Ceruloplasmin	10	4	3	0.3
F5GWX5	Chromodomain-helicase-DNA-binding protein 4	23	3	6	0.4
B4DJV2	Citrate synthase	56	18	3	0.6
F5H669	Cleavage and polyadenylation-specificity factor subunit 7	13	17	6	0.6
Q9NX63	Coiled-coil-helix-coiled-coil-helix domain-containing protein 3	15	15	4	0.4
Q9P0M6	Core histone macro-H2A.2	21	12	2	0.4
H3BSJ9	Cytochrome b-c1 complex subunit 2, mitochondrial	31	33	8	0.4
P47985	Cytochrome b-c1 complex subunit Rieske, mitochondrial	12	13	3	0.4
Q14204	Cytoplasmic dynein 1 heavy chain 1	51	6	23	0.4

TABLE III—*continued*

Accession	Description	Score	Coverage (%)	Unique Peptides	A2780-DR/A2780
Q9Y295	Developmentally-regulated GTP-binding protein 1	13	14	4	0.2
H0Y8E6	DNA replication licensing factor MCM2 (Fragment)	36	11	8	0.3
P33992	DNA replication licensing factor MCM5	28	12	8	0.4
E9PCY5	DNA topoisomerase 2 (Fragment)	61	16	9	0.5
P11388	DNA topoisomerase 2-alpha	89	16	14	0.4
E7EUY0	DNA-dependent protein kinase catalytic subunit	160	11	42	0.4
C9J4M6	DNA-directed RNA polymerase	22	5	6	0.5
B4DX52	DnaJ homolog subfamily B member 1	11	12	3	0.3
P49792	E3 SUM	11	3	8	0.5
Q9HC35	Echinoderm microtubule-associated protein-like 4	13	6	5	0.4
P68104	Elongation factor 1-alpha 1	345	34	6	0.5
E9PK01	Elongation factor 1-delta (Fragment)	15	27	5	0.2
Q9Y371	Endophilin-B1	10	14	5	0.3
P30040	Endoplasmic reticulum resident protein 29	32	38	8	0.5
P30084	Enoyl-CoA hydratase, mitochondrial	12	18	4	0.6
P05198	Eukaryotic translation initiation factor 2 subunit 1	16	15	5	0.2
F5H335	Eukaryotic translation initiation factor 3 subunit A	78	15	18	0.3
Q13347	Eukaryotic translation initiation factor 3 subunit I	11	13	4	0.2
P56537	Eukaryotic translation initiation factor 6	11	30	5	0.3
Q9NPD3	Exosome complex component RRP41	16	15	3	0.4
Q9Y5B9	FACT complex subunit SPT16	21	7	7	0.4
Q08945	FACT complex subunit SSRP1	45	16	12	0.6
P49327	Fatty acid synthase	98	14	28	0.3
P30043	Flavin reductase (NADPH)	11	31	4	0.5
P04075	Fructose-bisphosphatealdolase A	176	57	18	0.2
K7EQ48	Glucose-6-phosphate isomerase	45	16	8	0.5
B4DWJ2	Glutamine–tRNA ligase	17	11	8	0.5
O76003	Glutaredoxin-3	11	12	3	0.2
P78417	Glutathione S-transferase omega-1	28	14	3	0.4
P09211	Glutathione S-transferase P	15	25	4	0.4
P04406	Glyceraldehyde-3-phosphate dehydrogenase	247	55	16	0.2
H3BM42	Golgi apparatus protein 1	10	2	2	0.4
Q08379	Golgin subfamily A member 2	16	6	5	0.4
Q9UIJ7	GTP:AMP phosphotransferase AK3, mitochondrial	12	26	6	0.5
P62826	GTP-binding nuclear protein Ran	15	25	5	0.4
Q5T3Q7	HEAT repeat-containing protein 1	12	3	5	0.6
P07900	Heat shock protein HSP 90-alpha	716	55	24	0.5
P08238	Heat shock protein HSP 90-beta	925	56	24	0.5
D6R9P3	Heterogeneous nuclear ribonucleoprotein A/B	24	18	5	0.4
F8W6I7	Heterogeneous nuclear ribonucleoprotein A1	102	44	10	0.3
G3V4W0	Heterogeneous nuclear ribonucleoproteins C1/C2 (Fragment)	72	41	13	0.4
Q86YZ3	Hornerin	11	4	2	0.4
Q9Y4L1	Hypoxia up-regulated protein 1	182	39	33	0.5
P52292	Importin subunit alpha-1	17	10	6	0.6
Q12905	Interleukin enhancer-binding factor 2	68	22	7	0.5
P50213	Isocitrate dehydrogenase [NAD] subunit alpha, mitochondrial	27	26	8	0.3
O75874	Isocitrate dehydrogenase [NADP] cytoplasmic	15	16	6	0.2
B4DFL2	Isocitrate dehydrogenase [NADP]	19	19	6	0.4
Q9P2E9-2	Isoform 1 of Ribosome-binding protein 1	38	20	12	0.4
Q99714-2	Isoform 2 of 3-hydroxyacyl-CoA dehydrogenase type-2	51	54	8	0.5
Q92688-2	Isoform 2 of Acidic leucine-rich nuclear phosphoprotein 32	11	19	2	0.3
P23526-2	Isoform 2 of Adenosylhomocysteinase	13	7	3	0.3
O00571-2	Isoform 2 of ATP-dependent RNA helicase DDX3X	54	24	14	0.6
Q00610-2	Isoform 2 of Clathrin heavy chain 1	230	31	40	0.4
O15160-2	Isoform 2 of DNA-directed RNA polymerases I and III subunit	10	17	4	0.3
P21333-2	Isoform 2 of Filamin-A	385	29	56	0.4
P78347-2	Isoform 2 of General transcription factor II-I	57	13	12	0.5
P51991-2	Isoform 2 of Heterogeneous nuclear ribonucleoprotein A3	39	22	6	0.5
P31942-2	Isoform 2 of Heterogeneous nuclear ribonucleoprotein H3	25	17	4	0.3
Q86UP2-2	Isoform 2 of Kinectin	66	15	17	0.4
Q9NZM1-2	Isoform 2 of Myoferlin	35	7	12	0.5
P12036-2	Isoform 2 of Neurofilament heavy polypeptide	94	8	5	0.4
Q9Y617-2	Isoform 2 of Phosphoserine aminotransferase	14	17	5	0.2
P11940-2	Isoform 2 of Polyadenylate-binding protein 1	70	31	15	0.6

TABLE III—*continued*

Accession	Description	Score	Coverage (%)	Unique Peptides	A2780-DR/A2780
O75400-2	Isoform 2 of Pre-mRNA-processing factor 40 homolog A	19	10	7	0.4
P28370-2	Isoform 2 of Probable global transcription activator SNF2L1	42	9	2	0.4
P25788-2	Isoform 2 of Proteasome subunit alpha type-3	24	24	6	0.3
Q5VT52-2	Regulation of nuclear pre-mRNA domain-containing protein 2	10	5	5	0.5
Q92900-2	Isoform 2 of Regulator of nonsense transcripts 1	18	7	6	0.4
Q5JTH9-2	Isoform 2 of RRP12-like protein	24	8	8	0.5
P16615-2	Sarcoplasmic/endoplasmic reticulum calcium ATPase 2	43	15	12	0.5
Q9H2G2-2	Isoform 2 of STE20-like serine/threonine-protein kinase	11	4	5	0.4
A6NHR9-2	Structural maintenance of CFH domain-containing protein 1	15	2	4	0.3
O14776-2	Isoform 2 of Transcription elongation regulator 1	15	4	6	0.4
P60174-1	Isoform 2 of Triosephosphateisomerase	112	62	14	0.3
P07951-2	Isoform 2 of Tropomyosin beta chain	21	20	4	0.2
O43399-2	Isoform 2 of Tumor protein D54	19	31	4	0.4
Q9UIG0-2	Isoform 2 of Tyrosine-protein kinase BAZ1B	33	9	12	0.4
Q9NYU2-2	Isoform 2 of UDP-glucose:glycoproteinglucosyltransferase 1	27	7	8	0.6
P30622-2	Isoform 3 of CAP-Gly domain-containing linker protein 1	16	4	6	0.4
Q9Y281-3	Isoform 3 of Cofilin-2	11	18	2	0.3
P33993-3	Isoform 3 of DNA replication licensing factor MCM7	18	17	7	0.6
Q14103-3	Isoform 3 of Heterogeneous nuclear ribonucleoprotein D0	23	27	7	0.4
P06756-3	Isoform 3 of Integrin alpha-V	111	25	23	0.5
Q7L2E3-3	Isoform 3 of Putative ATP-dependent RNA helicase DHX30	22	8	8	0.4
P08559-3	Pyruvate dehydrogenase E1 component subunit alpha,	18	14	5	0.4
Q13813-3	Isoform 3 of Spectrin alpha chain, non-erythrocytic 1	135	16	34	0.4
Q99832-3	Isoform 3 of T-complex protein 1 subunit eta	75	36	14	0.5
Q86W42-3	Isoform 3 of TH	11	24	5	0.3
Q14669-4	Isoform 4 of E3 ubiquitin-protein ligase TRIP12	18	4	5	0.4
Q8N766-4	Isoform 4 of ER membrane protein complex subunit 1	14	5	3	0.5
P54819-5	Isoform 5 of Adenylate kinase 2, mitochondrial	16	30	5	0.3
O75369-6	Isoform 6 of Filamin-B	48	5	8	0.5
P27816-6	Isoform 6 of Microtubule-associated protein 4	25	10	10	0.4
Q04637-7	Isoform 7 of Eukaryotic translation initiation factor 4 gamma 1	29	8	11	0.3
Q15149-7	Isoform 7 of Plectin	99	9	34	0.4
Q00325-2	Isoform B of Phosphate carrier protein, mitochondrial	40	15	6	0.4
P02788-2	Isoform DeltaLf of Lactotransferrin	22	8	5	0.4
P31946-2	Isoform Short of 14–3-3 protein beta/alpha	48	36	3	0.3
P46013-2	Isoform Short of Antigen KI-67	20	4	8	0.5
O75534-2	Isoform Short of Cold shock domain-containing protein E1	11	9	6	0.6
Q15056-2	Isoform Short of Eukaryotic translation initiation factor 4H	10	29	5	0.3
J3KR24	Isoleucine–tRNA ligase, cytoplasmic	25	6	7	0.3
P42704	Leucine-rich PPR motif-containing protein, mitochondrial	334	32	43	0.5
P00338	L-lactate dehydrogenase A chain	15	9	2	0.4
P07195	L-lactate dehydrogenase B chain	14	9	2	0.5
O00264	Membrane-associated progesterone receptor component 1	17	16	3	0.6
B4E1E9	Mitochondrial dicarboxylate carrier	12	19	5	0.5
Q9BQG0	Myb-binding protein 1A	60	15	18	0.5
P19105	Myosin regulatory light chain 12A	13	19	3	0.5
P35580	Myosin-10	36	5	3	0.4
P35579	Myosin-9	163	20	28	0.4
O75489	NADH dehydrogenase [ubiquinone] iron-sulfur protein 3	26	33	7	0.5
P48681	Nestin	40	9	13	0.4
Q09666	Neuroblast differentiation-associated protein AHNAK	17	5	7	0.4
P69849	Nodal modulator 3	25	9	9	0.5
Q14980	Nuclear mitotic apparatus protein 1	130	22	39	0.6
P49790	Nuclear pore complex protein Nup153	16	6	7	0.6
E9PF10	Nuclear pore complex protein Nup155	14	5	6	0.6
Q92621	Nuclear pore complex protein Nup205	20	4	9	0.5
Q8TEM1	Nuclear pore membrane glycoprotein 210	21	6	8	0.5
Q14978	Nucleolar and coiled-body phosphoprotein 1	28	17	10	0.5
P06748	Nucleophosmin	113	46	13	0.3
P12270	Nucleoprotein TPR	82	12	28	0.6
Q02790	Peptidyl-prolylcis-trans isomerase FKBP4	36	25	10	0.5
P32119	Peroxiredoxin-2	45	26	5	0.5
H7C3T4	Peroxiredoxin-4 (Fragment)	36	39	4	0.5
P30041	Peroxiredoxin-6	49	24	6	0.3

TABLE III—*continued*

Accession	Description	Score	Coverage (%)	Unique Peptides	A2780-DR/A2780
O95571	Persulfidedioxygenase ETHE1, mitochondrial	12	16	3	0.4
P00558	Phosphoglycerate kinase 1	37	30	10	0.2
P18669	Phosphoglyceratemutase 1	71	43	9	0.3
E9PBS1	Phosphoribosylaminoimidazole carboxylase (Fragment)	10	9	3	0.4
O15067	Phosphoribosylformylglycinamidine synthase	10	6	5	0.3
Q15102	Platelet-activating factor acetylhydrolase IB subunit gamma	24	22	5	0.3
Q15365	Poly(rC)-binding protein 1	35	28	4	0.2
H3BRU6	Poly(rC)-binding protein 2 (Fragment)	33	30	4	0.3
O75915	PRA1 family protein 3	13	16	2	0.4
Q6P2Q9	Pre-mRNA-processing-splicing factor 8	61	11	21	0.4
Q8IY81	pre-rRNA processing protein FTSJ3	19	8	7	0.4
P07737	Profilin-1	95	65	9	0.4
P25789	Proteasome subunit alpha type-4	14	16	5	0.3
P28066	Proteasome subunit alpha type-5	18	23	4	0.3
P60900	Proteasome subunit alpha type-6	42	35	9	0.2
P20618	Proteasome subunit beta type-1	17	17	4	0.4
J3KSM3	Proteasome subunit beta type-3	15	23	2	0.4
P28070	Proteasome subunit beta type-4	20	19	4	0.2
P28074	Proteasome subunit beta type-5	11	17	4	0.5
P28072	Proteasome subunit beta type-6	19	13	3	0.4
Q99436	Proteasome subunit beta type-7	11	18	4	0.3
Q14690	Protein RRP5 homolog	12	3	5	0.5
Q99584	Protein S100-A13	23	48	5	0.6
P05109	Protein S100-A8	11	40	4	0.6
P06702	Protein S100-A9	22	38	4	0.4
P14618	Pyruvate kinase PKM	371	64	32	0.7
P46940	RasGTPase-activating-like protein IQGAP1	65	13	18	0.5
Q15907	Ras-related protein Rab-11B	48	39	9	0.6
P61106	Ras-related protein Rab-14	26	25	4	0.3
P62820	Ras-related protein Rab-1A	37	36	6	0.5
B4DJA5	Ras-related protein Rab-5A	13	21	2	0.4
P51148	Ras-related protein Rab-5C	26	19	2	0.3
J3QR09	Ribosomal protein L19	16	21	4	0.1
P38159	RNA-binding motif protein, X chromosome	61	44	17	0.6
P49756	RNA-binding protein 25	11	7	4	0.4
Q5QPM1	RNA-binding protein Raly (Fragment)	16	27	5	0.5
Q14151	Scaffold attachment factor B2	18	4	2	0.5
P35270	Sepiapterin reductase	14	33	6	0.4
B5MCX3	Septin-2	15	25	6	0.2
B4E241	Serine/arginine-rich-splicing factor 3	21	25	3	0.6
P62136	Serine/threonine-protein phosphatase PP1-alpha catalytic	21	25	3	0.3
P02768	Serum albumin	123	43	25	0.4
Q9Y5M8	Signal recognition particle receptor subunit beta	11	14	3	0.4
J3QLE5	Small nuclear ribonucleoprotein-associated protein N	21	26	4	0.3
Q01082	Spectrin beta chain, non-erythrocytic 1	62	10	21	0.5
O75533	Splicing factor 3B subunit 1	93	19	21	0.4
Q13435	Splicing factor 3B subunit 2	40	10	8	0.6
Q15393	Splicing factor 3B subunit 3	56	10	10	0.5
B4E1K7	Stomatin-like protein 2, mitochondrial	36	32	7	0.5
Q14683	Structural maintenance of chromosomes protein 1A	20	5	7	0.4
Q9UQE7	Structural maintenance of chromosomes protein 3	12	5	5	0.4
Q6UWP8	Suprabasin	17	15	2	0.4
O60264	SWI/SNF-related matrix-associated actin-dependent regulator	73	16	9	0.5
Q92797	Symplekin	11	4	4	0.5
Q5TCU6	Talin-1	39	6	12	0.4
P17987	T-complex protein 1 subunit alpha	85	40	19	0.6
P40227	T-complex protein 1 subunit zeta	97	33	15	0.5
Q9BRA2	Thioredoxin domain-containing protein 17	17	33	4	0.5
E9PH29	Thioredoxin-dependent peroxide reductase, mitochondrial	73	26	6	0.6
Q8NI27	TH	14	5	8	0.4
Q9Y2W1	Thyroid hormone receptor-associated protein 3	35	13	10	0.3
P37837	Transaldolase	19	13	5	0.3

TABLE III—*continued*

Accession	Description	Score	Coverage (%)	Unique Peptides	A2780-DR/A2780
Q01995	Transgelin	13	35	6	0.4
P37802	Transgelin-2	15	23	4	0.5
Q92616	Translational activator GCN1	31	5	11	0.4
P09661	U2 small nuclear ribonucleoprotein A'	26	31	7	0.5
P08579	U2 small nuclear ribonucleoprotein B''	17	24	5	0.4
O75643	U5 small nuclear ribonucleoprotein 200 kDa helicase	67	10	18	0.5
P09936	Ubiquitin carboxyl-terminal hydrolase isozyme L1	22	26	6	0.3
D6RDM7	Ubiquitin-conjugating enzyme E2 K (Fragment)	13	22	2	0.5
P54727	UV excision repair protein RAD23 homolog B	18	18	7	0.5
P26640	Valine–tRNA ligase	13	4	4	0.4
O75396	Vesicle-trafficking protein SEC22b	15	15	3	0.4
Q00341	Vigilin	25	8	8	0.4
P08670	Vimentin	1987	81	43	0.4
P13010	X-ray repair cross-complementing protein 5	58	17	11	0.6

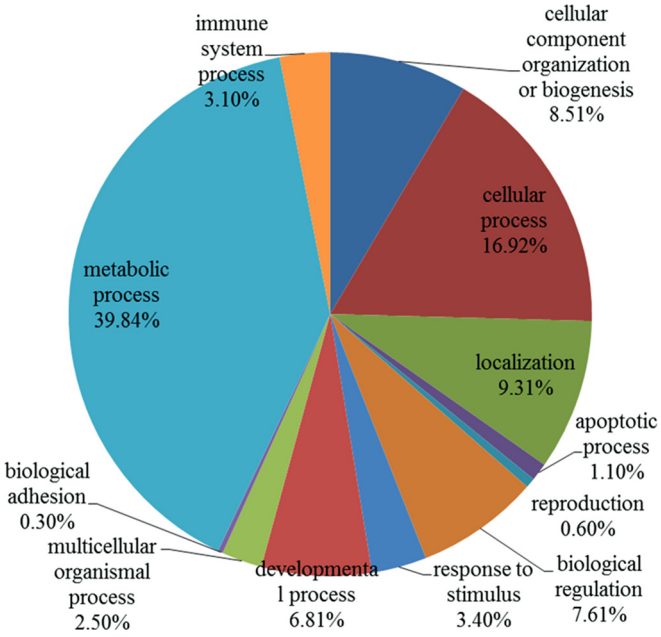

FIG. 3. **Functional classification of differentially expressed proteins between A2780 and A2780-DR cells with PANTHER (http://www.pantherdb.org).**

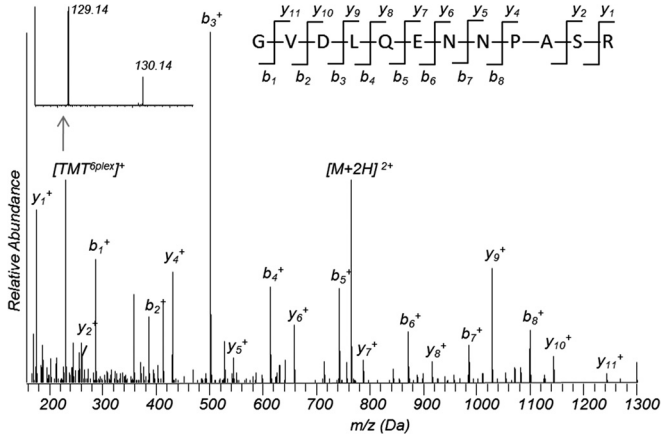

FIG. 4. **MS/MS spectra for identification of Rab 5C: A MS/MS spectrum of a doubly charged TMT-labeled peptide ion at *m/z* 764.** 9025 for MH_2^{2+} corresponding to the mass of the peptide GVDLQENNPASR from Rab 5C. Fig. inserts show peaks of TMT reporter ions of two labeled peptides.

was only one third of that in A2780 cells, suggesting that a reduction in cellular Pt accumulation is the major cause of drug-resistance in A2780-DR cells.

To identify factors leading to drug resistance, we used TMT labeling to quantify proteins from two types of cells. TMT-labeling uses an isobaric tag with an amine-reactive NHS-ester group, which enables quantitation of two samples with a single LC-MS/MS run that eliminates experimental variation. It also enhances the ionization efficiency of peptides to make them more amenable for MS analysis. We identified about 1900 proteins in three repeated experiments. Among them, 340 proteins were differentially expressed between A2780 and A2780-DR cells, which participate in a variety of cellular processes including cell metabolism, stress responses, cell cycle, and DNA repair. Based on GO analysis, 135 proteins are associated with the metabolic processes including ferredoxin metabolic process (GO:0006124); nitrogen compound metabolic process (GO:0006807); oxygen and reactive oxygen species metabolic process (GO:0006800); phosphate metabolic process (GO:0006796); and primary metabolic process (GO:0044238).

Five out of ten glycolytic proteins were down-regulated including Glucose-6-phosphate isomerase (GPI), fructose-bisphosphate aldolase (ALDO), lactate dehydrogenase (LDH), PGK, and pyruvate kinase (PKM), indicating that glycolysis was down-regulated in drug-resistant cells. This is consistent with an earlier report showing that ALDO and PGK are down-regulated in drug-resistant cells (32). The other proteomic study has also linked the decreased pyruvate kinase M2 expression to oxaliplatin resistance in patients with colorectal cancer, showing tumors with the lowest PKM2 levels attain the lowest oxaliplatin response rates and the high PKM2 levels are associated with high p53 levels (44). In the present study, the expression level of PKM in A2780-DR cells was about half of that in A2780 cells (Table III) by quantitative

proteomic analysis. This was confirmed by Western blotting (Fig. 5). The mRNA level of PKM2 in A2780-DR cells was also down-regulated compared with A2780 cells by qPCR analysis. PKM2 catalyzes the rate-limiting step of glycolysis, in which phosphoenolpyruvate is converted to pyruvate. As a key enzyme for cancer metabolism and tumor growth, PKM2 and other glycolytic enzymes were found to be up-regulated in most cancer cells (45–47). However, our results and previous studies have shown that down-regulation of glycolytic enzymes are a characteristic of drug-resistant ovarian cancer and colorectal cancer cells (32, 44). Although the molecular events leading to down-regulation of glycolytic enzymes are still not clear, we have found that expression levels of c-Myc and HIF1A are down-regulated in drug-resistant cells. Western blots of c-Myc and HIF1A are displayed in supplemental Fig. S2, showing that both c-Myc and HIF1a are down-regulated in A2780-DR cells. c-Myc is an oncogene that regulates transcription of many growth related genes. HIF1A is a master transcriptional regulator of the adaptive response to hypoxia that activates the transcription of glycolytic enzymes. Down-regulation of c-Myc and HIF1A results in decreases in expression levels of glycolytic enzymes that may contribute to drug resistance in ovarian cancer cells.

Cisplatin is a potent electrophile covalently modifying nucleophilic sites on proteins, lipids, DNA, and RNA to generate reactive oxygen species and to induce cell apoptosis. To explore the difference in endogenous ROS levels between A280 and A2780-DR, the intracellular ROS levels were measured with the Image-iT™ LIVE Green Reactive Oxygen Species Detection Kit in both cells. Results show that the ROS level in A2780-DR cells is lower than that in A2780 cells (supplemental Fig. S3), indicating that A2780_DR cells possess a higher capacity to accommodate cisplatin-induced ROS stress. However, quantitative proteomics showed that some redox proteins such as peroxiredoxin-6 (PRDX6) and thioredoxin reductase 1 (TR1) were down-regulated, whereas glutathione reductase (GSR) is up-regulated in A2780-DR cells (Table II). GSR maintains high levels of reduced glutathione in the cytosol, and the up-regulation of GSR may lead to a decrease of ROS in A2780-DR cells. Studies are underway to understand the complex interactions of ROS and the cellular antioxidant system.

On 1D SDS-PAGE (Fig. 2), band 7 has the largest change in intensity, in which vimentin was identified as the major protein. Quantitative proteomics showed that expression of vimentin was decreased 2-fold in A2780-DR cells as compared with A2780 cells, which was confirmed by Western blotting (Fig. 5*A*). Vimentin is a major intermediate filament protein and is ubiquitously expressed to maintain cellular integrity. Overexpression of vimentin has been observed in various epithelial cancers and correlated with accelerated tumor growth, invasion, and poor prognosis (50). Furthermore, etoposide resistance in neuroblastoma cell and vinca alkaloid resistance in acute lymphoblastic leukemia have been linked to overexpression of vimentin (51–52). However, down-regulation of

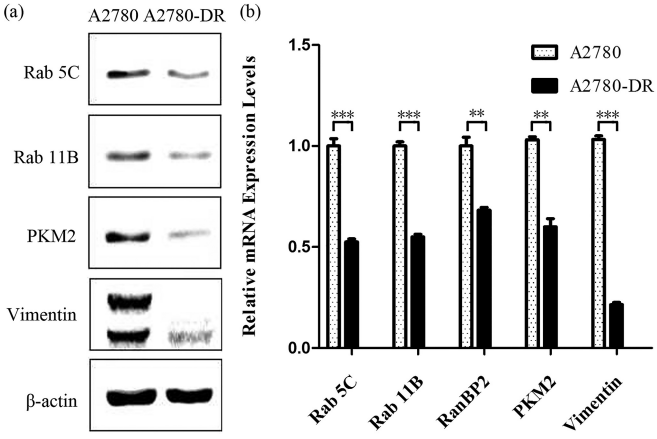

FIG. 5. **Confirmation of differentially expressed proteins by Western and qPCR.** *A*, Western blot analysis of selected proteins from A2780 and A2780-DR cells. *B*, qPCR analysis of selected genes from A2780 and A2780-DR cells. ** for p value <0.001; and *** for p value <0.001.

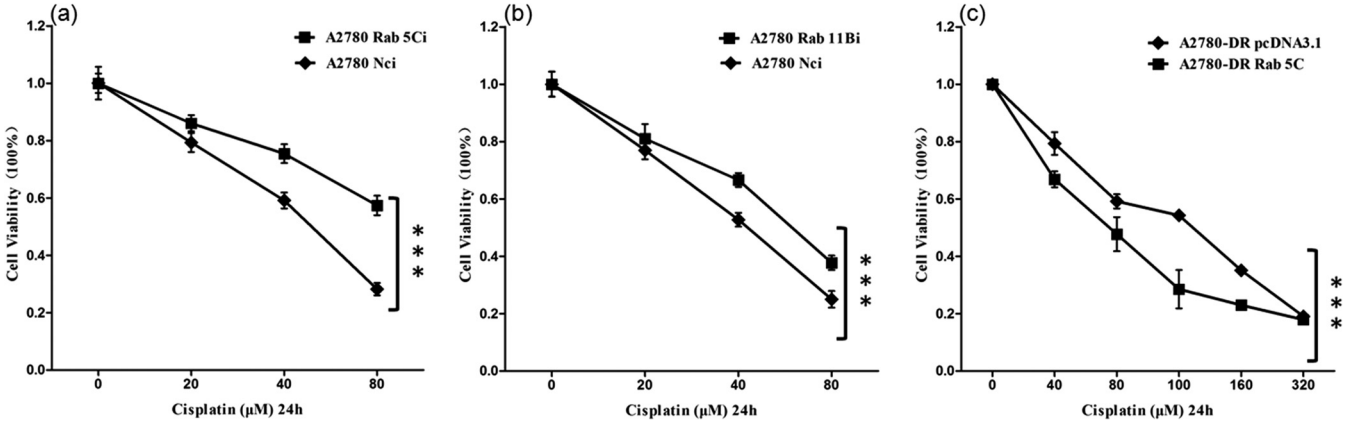

FIG. 6. **Cell cytotoxicity assays.** Percentage of viable A2780, shRNA-transfected A2780, and Rab 5C-pcDNA3.1-transfected cells treated with cisplatin at different concentrations for 24 h determined by using CCK-8 assay. Results are expressed as the mean of three experiments; *A,* Rab 5Ci; *B*, Rab 11Bi; and *C*, Rab 5C-pcDNA3.1. ***$p < 0.001$.

vimentin has been found in resistant1A9 cells to the microtubule stabilizing agents, PLA and LAU (53), consistent with results from the present study. Therefore, changes in expression levels of vimentin are cancer-type dependent and vimentin is a potential marker for drug-resistance in ovarian cancer.

Decreased cellular drug accumulation is the most commonly observed phenomenon among drug resistant cells. In the present study, we found that cisplatin accumulation was lower in drug-resistant cells (Fig. 1). It is known that cisplatin was not a substrate of P-glycoprotein the key mediator for drug efflux (10–13). Therefore, reduction of cisplatin accumulation in drug-resistant cells may be related to uptake of cisplatin. Uptake of cisplatin can be governed by different mechanisms including passive diffusion, carrier-mediated transporting, and endocytosis (54). An elegant study has shown that several small GTPases (Rab 5, Rac 1, and Rho A) were down-regulated in cisplatin-resistant human hepatoma and epidermal carcinoma cells, demonstrating that GTPase-regulated endocytosis is an important factor in drug-resistance (55). Quantitative proteomic analysis in this study shows that Ras-related proteins Rab 5C and Rab 11B are down-regulated in A2780-DR cells as confirmed by Western blotting and qPCR. Rab 5C is a member of the Rab protein family and a key regulator in endocytosis and early endosome fusion, whereas Rab 11 has been associated with endosome recycling (56). Therefore, down-regulation of Rab 5C and Rab 11B may result in reduced accumulation of cisplatin. To further confirm Rab 5C and Rab 11B mediated drug-resistance, shRNAs against Rab 5C and Rab 11B were used to silence these genes in A2780 cells. As predicted, silencing Rab 5C in A2780 cells lead to increased drug resistance (Fig. 6), but effects of Rab 11B shRNA are less significant (Table I). On the other hand, overexpression of Rab5C in A2780-DR cells increases its sensitivity to cisplatin treatment. These results suggest for the first time that Rab 5C mediated endocytosis regulates drug resistance in ovarian cancer cells.

CONCLUSIONS

Taken together, our results show that multiple cellular processes contribute to drug resistance in ovarian cancer cells. Although increased glycolysis is observed in most cancer cells, glycolytic enzymes PKM2, GPI, ALDO, LDH, and PGK are down-regulated in drug-resistant ovarian cancer cells. Drug resistance is also associated with a decrease of the endogenous ROS level, the up-regulation of GSR, as well as down-regulation of vimentin. Furthermore, the down-regulation of Rab 5C-mediated endocytosis contributes to the reduction of cellular cisplatin accumulation and drug-resistance. These results further our understanding of the multifactorial mechanisms in acquisition and development of cisplatin resistance in human cancer cells.

Acknowledgments—We thank the Protein Chemistry Facility at the Center for Biomedical Analysis of Tsinghua University for sample analysis. We thank Dr Zhenyu Zhang for valuable discussions.

* This work was supported in part by NSFC 30871434 (R.S.G.) and NSFC 31270871 (H.T.D), the Chinese Ministry of Science and Technology 2014CBA02005 (H.T.D) and the Global Science Alliance Program of Thermo-Fisher Scientific.

S This article contains supplemental Figs. S1 to S3 and Tables S1 to S3.

‖ To whom correspondence should be addressed: School of Life Sciences, Tsinghua University, HaiDianQu, Beijing, 100084 China. Tel.: 8610-62790498; Fax: 8610-62797154; E-mail: dht@mail.tsinghua.edu.cn.

** These authors contribute equally to this work.

REFERENCES

1. Bell, D., Berchuck, A., Birrer, M., Chien, J., Cramer, D., Dao, F., Dhir, R., Disaia, P., Gabra, H., and Glenn, P. (2011) Integrated genomic analyses of ovarian carcinoma. *Nature* **474,** 609–615
2. Miller, D. S., Blessing, J. A., Krasner, C. N., Mannel, R. S., Hanjani, P., Pearl, M. L., Waggoner, S. E., and Boardman, C. H. (2009) Phase II evaluation of pemetrexed in the treatment of recurrent or persistent platinum-resistant ovarian or primary peritoneal carcinoma: a study of the Gynecologic Oncology Group. *J. Clin. Oncol.* **27,** 2686–2691
3. Jemal, A., Siegel, R., Ward, E., Hao, Y., Xu, J., and Thun, M. J. (2009) Cancer statistics, 2009. *CA Cancer J. Clin.* **59,** 225–249
4. Fojo, A., Hamilton, T. C., Young, R. C., and Ozols, R. F. (1987) Multidrug resistance in ovarian cancer. *Cancer* **60,** 2075–2080
5. Safaei, R., and Howell, S. B. (2005) Copper transporters regulate the cellular pharmacology and sensitivity to Pt drugs. *Crit. Rev. Oncol. Hemat.* **53,** 13–23
6. Ishida, S., Lee, J., Thiele, D. J., and Herskowitz, I. (2002) Uptake of the anticancer drug cisplatin mediated by the copper transporter Ctr1 in yeast and mammals. *Proc. Natl. Acad. Sci.* **99,** 14298–14302
7. Safaei, R., Katano, K., Samimi, G., Naerdemann, W., Stevenson, J. L., Rochdi, M., and Howell, S. B. (2004) Cross-resistance to cisplatin in cells with acquired resistance to copper. *Cancer Chemoth. Pharm.* **53,** 239–246
8. Lin, X., Okuda, T., Holzer, A., and Howell, S. B. (2002) The copper transporter CTR1 regulates cisplatin uptake in *Saccharomyces cerevisiae*. *Mol. Pharmacol.* **62,** 1154–1159
9. Holzer, A. K., Katano, K., Klomp, L. W., and Howell, S. B. (2004) Cisplatin rapidly down-regulates its own influx transporter hCTR1 in cultured human ovarian carcinoma cells. *Clin. Cancer Res.* **10,** 6744–6749
10. Breier, A., Gibalova, L., Seres, M., Barancik, M., and Sulova, Z. (2013) New Insight into P-glycoprotein as a drug target. *Anti-Cancer Agent. Me.* **13,** 159–170
11. Cocker, H. A., Tiffin, N., Pritchard-Jones, K., Pinkerton, C. R., and Kelland, L. R. (2001) *In vitro* prevention of the emergence of multidrug resistance in a pediatric rhabdomyosarcoma cell line. *Clin. Cancer Res.* **7,** 3193–3198
12. Yang, X., and Page, M. (1995) P-glycoprotein expression in ovarian cancer cell line following treatment with cisplatin. *Oncol. Res.* **7,** 619–624
13. Stordal, B., Hamon, M., McEneaney, V., Roche, S., Gillet, J.-P., O'Leary, J. J., Gottesman, M., and Clynes, M. (2012) Resistance to paclitaxel in a cisplatin-resistant ovarian cancer cell line is mediated by P-glycoprotein. *PLoS One* **7,** e40717
14. Kelland, L. (2007) The resurgence of platinum-based cancer chemotherapy. *Nat. Rev. Cancer* **7,** 573–584
15. Sakamoto, M., Kondo, A., Kawasaki, K., Goto, T., Sakamoto, H., Miyake, K., Koyamatsu, Y., Akiya, T., Iwabuchi, H., and Muroya, T. (2001) Analysis of gene expression profiles associated with cisplatin resistance in human ovarian cancer cell lines and tissues using cDNA microarray. *Human Cell* **14,** 305–315
16. Li, M., Balch, C., Montgomery, J. S., Jeong, M., Chung, J. H., Yan, P., Huang, T. H., Kim, S., and Nephew, K. P. (2009) Integrated analysis of DNA methylation and gene expression reveals specific signaling pathways associated with platinum resistance in ovarian cancer. *BMC Med. Genomics* **2,** 34
17. Godwin, A. K., Meister, A., O'Dwyer, P. J., Huang, C. S., Hamilton, T. C., and Anderson, M. E. (1992) High resistance to cisplatin in human ovarian cancer cell lines is associated with marked increase of glutathione synthesis. *Proc. Natl. Acad. Sci.* **89,** 3070–3074
18. Hector, S., Nava, M. E., Clark, K., Murphy, M., and Pendyala, L. (2007)

Characterization of a clonal isolate of an oxaliplatin resistant ovarian carcinoma cell line A2780/C10. *Cancer Lett.* **245,** 195–204
19. Martin, L. P., Hamilton, T. C., and Schilder, R. J. (2008) Platinum resistance: the role of DNA repair pathways. *Clin. Cancer Res.* **14,** 1291–1295
20. Selvakumaran, M., Pisarcik, D. A., Bao, R., Yeung, A. T., and Hamilton, T. C. (2003) Enhanced cisplatin cytotoxicity by disturbing the nucleotide excision repair pathway in ovarian cancer cell lines. *Cancer Res.* **63,** 1311–1316
21. Dabholkar, M., Vionnet, J., Bostick-Bruton, F., Yu, J. J., and Reed, E. (1994) Messenger RNA levels of XPAC and ERCC1 in ovarian cancer tissue correlate with response to platinum-based chemotherapy. *J. Clin. Invest.* **94,** 703–708
22. Kohn, E. C., Sarosy, G., Bicher, A., Link, C., Christian, M., Steinberg, S. M., Rothenberg, M., Adamo, D. O., Davis, P., and Ognibene, F. P. (1994) Dose-intense taxol: high response rate in patients with platinum-resistant recurrent ovarian cancer. *J. Natl. Cancer I.* **86,** 18–24
23. Murphy, M. A., and Wentzensen, N. (2011) Frequency of mismatch repair deficiency in ovarian cancer: a systematic review. *Int. J. Cancer* **129,** 1914–1922
24. Sakai, W., Swisher, E. M., Karlan, B. Y., Agarwal, M. K., Higgins, J., Friedman, C., Villegas, E., Jacquemont, C., Farrugia, D. J., and Couch, F. J. (2008) Secondary mutations as a mechanism of cisplatin resistance in BRCA2-mutated cancers. *Nature* **451,** 1116–1120
25. Edwards, S. L., Brough, R., Lord, C. J., Natrajan, R., Vatcheva, R., Levine, D. A., Boyd, J., Reis-Filho, J. S., and Ashworth, A. (2008) Resistance to therapy caused by intragenic deletion in BRCA2. *Nature* **451,** 1111–1115
26. Swisher, E. M., Sakai, W., Karlan, B. Y., Wurz, K., Urban, N., and Taniguchi, T. (2008) Secondary BRCA1 mutations in BRCA1-mutated ovarian carcinomas with platinum resistance. *Cancer Res.* **68,** 2581–2586
27. Ali, A. Y., Farrand, L., Kim, J. Y., Byun, S., Suh, J. Y., Lee, H. J., and Tsang, B. K. (2012) Molecular determinants of ovarian cancer chemoresistance: new insights into an old conundrum. *Ann. NY Acad. Sci.* **1271,** 58–67
28. Stronach, E. A., Chen, M., Maginn, E. N., Agarwal, R., Mills, G. B., Wasan, H., and Gabra, H. (2011) DNA-PK mediates AKT activation and apoptosis inhibition in clinically acquired platinum resistance. *Neoplasia* **13,** 1069–1080
29. Stronach, E. A., Alfraidi, A., Rama, N., Datler, C., Studd, J. B., Agarwal, R., Guney, T. G., Gourley, C., Hennessy, B. T., and Mills, G. B. (2011) HDAC4-regulated STAT1 activation mediates platinum resistance in ovarian cancer. *Cancer Res.* **71,** 4412–4422
30. Yan, X., Pan, L., Yuan, Y., Lang, J., and Mao, N. (2007) Identification of platinum-resistance associated proteins through proteomic analysis of human ovarian cancer cells and their platinum-resistant sublines. *J. Proteome Res.* **6,** 772–780
31. Jinawath, N., Vasoontara, C., Jinawath, A., Fang, X., Zhao, K., Yap, K.-L., Guo, T., Lee, C. S., Wang, W., and Balgley, B. M. (2010) Oncoproteomic analysis reveals co-upregulation of RELA and STAT5 in carboplatin resistant ovarian carcinoma. *PLoS One* **5,** e11198
32. Gong, F., Peng, X., Zeng, Z., Yu, M., Zhao, Y., and Tong, A. (2011) Proteomic analysis of cisplatin resistance in human ovarian cancer using 2-DE method. *Mol. Cell. Biochem.* **348,** 141–147
33. Di Michele, M., Della Corte, A., Cicchillitti, L., Del Boccio, P., Urbani, A., Ferlini, C., Scambia, G., Donati, M. B., and Rotilio, D. (2009) A proteomic approach to paclitaxel chemoresistance in ovarian cancer cell lines. *Biochim. Biophys. Acta* **1794,** 225–236
34. Stewart, J. J., White, J. T., Yan, X., Collins, S., Drescher, C. W., Urban, N. D., Hood, L., and Lin, B. (2006) Proteins associated with Cisplatin resistance in ovarian cancer cells identified by quantitative proteomic technology and integrated with mRNA expression levels. *Mol. Cell. Proteomics* **5,** 433–443
35. Cicchillitti, L., Di Michele, M., Urbani, A., Ferlini, C., Donati, M. B., Scambia, G., and Rotilio, D. (2009) Comparative proteomic analysis of paclitaxel sensitive A2780 epithelial ovarian cancer cell line and its resistant counterpart A2780TC1 by 2D-DIGE: the role of ERp57. *J. Proteome Res.* **8,** 1902–1912
36. Yang, Z., Schumaker, L. M., Egorin, M. J., Zuhowski, E. G., Guo, Z., and Cullen, K. J. (2006) Cisplatin preferentially binds mitochondrial DNA and voltage-dependent anion channel protein in the mitochondrial membrane of head and neck squamous cell carcinoma: possible role in apoptosis. *Clin. Cancer Res.* **12,** 5817–5825
37. Custódio, J., Cardoso, C. M., Santos, M. S., Almeida, L. M., Vicente, J. A., and Fernandes, M. A. (2009) Cisplatin impairs rat liver mitochondrial functions by inducing changes on membrane ion permeability: prevention by thiol group protecting agents. *Toxicology* **259,** 18–24
38. Saitou, M., Isonishi, S., Hamada, T., Kiyokawa, T., Tachibana, T., Ishikawa, H., and Yasuda, M. (2009) Mitochondrial ultrastructure-associated chemotherapy response in ovarian cancer. *Oncology Reports* **21,** 199–204
39. Liang, X., Finkel, T., Shen, D., Yin, J., Aszalos, A., and Gottesman, M. M. (2008) SIRT1 contributes in part to cisplatin resistance in cancer cells by altering mitochondrial metabolism. *Mol. Cancer Res,* **6,** 1499–1506
40. Andrews, P. A., and Albright, K. D. (1992) Mitochondrial defects in cis-diamminedichloroplatinum (II)-resistant human ovarian carcinoma cells. *Cancer Res.* **52,** 1895–1901
41. Dai, Z., Yin, J., He, H., Li, W., Hou, C., Qian, X., Mao, N., and Pan, L. (2010) Mitochondrial comparative proteomics of human ovarian cancer cells and their platinum-resistant sublines. *Proteomics* **10,** 3789–3799
42. Chappell, N. P., Teng, P.-n., Hood, B. L., Wang, G., Darcy, K. M., Hamilton, C. A., Maxwell, G. L., and Conrads, T. P. (2012) Mitochondrial proteomic analysis of cisplatin resistance in ovarian cancer. *J. Proteome Res.* **11,** 4605–4614
43. Minakata, K., Nozawa, H., Okamoto, N., and Suzuki, O. (2006) Determination of platinum derived from cisplatin in human tissues using electrospray ionization mass spectrometry. *J. Chromatogr. B* **832,** 286–291
44. Martinez-Balibrea, E., Plasencia, C., Ginés, A., Martinez-Cardús, A., Musulén, E., Aguilera, R., Manzano, J. L., Neamati, N., and Abad, A. (2009) A proteomic approach links decreased pyruvate kinase M2 expression to oxaliplatin resistance in patients with colorectal cancer and in human cell lines. *Mol. Cancer Ther.* **8,** 771–778
45. Christofk, H. R., Vander Heiden, M. G., Harris, M. H., Ramanathan, A., Gerszten, R. E., Wei, R., Fleming, M. D., Schreiber, S. L., and Cantley, L. C. (2008) The M2 splice isoform of pyruvate kinase is important for cancer metabolism and tumour growth. *Nature* **452,** 230–233
46. Mazurek, S. (2012) Pyruvate kinase M2: a key enzyme of the tumor metabolome and its medical relevance. *Biomedical Res.* **23,** 133–141
47. Xu, R., Pelicano, H., Zhou, Y., Carew, J. S., Feng, L., Bhalla, K. N., Keating, M. J., and Huang, P. (2005) Inhibition of glycolysis in cancer cells: a novel strategy to overcome drug resistance associated with mitochondrial respiratory defect and hypoxia. *Cancer Res.* **65,** 613–621
48. Chung, Y., Yoo, Y., Park, J., Kim, Y., and Kim, H. J. (2000) Increased expression of peroxiredoxin II confers resistance to cisplatin. *Anticancer Res.* **21,** 1129–1133
49. Pak, J. H., Choi, W. H., Lee, H. M., Joo, W.-D., Kim, J.-H., Kim, Y.-T., Kim, Y.-M., and Nam, J.-H. (2011) Peroxiredoxin 6 overexpression attenuates cisplatin-induced apoptosis in human ovarian cancer cells. *Cancer Invest.* **29,** 21–28
50. Satelli, A., and Li, S. (2011) Vimentin in cancer and its potential as a molecular target for cancer therapy. *Cell. Mol. Life Sci.* **68,** 3033–3046
51. Verrills, N. M., Walsh, B. J., Cobon, G. S., Hains, P. G., and Kavallaris, M. (2003) Proteome analysis of vinca alkaloid response and resistance in acute lymphoblastic leukemia reveals novel cytoskeletal alterations. *J. Biol. Chem.* **278,** 45082–45093
52. Urbani, A., Poland, J., Bernardini, S., Bellincampi, L., Biroccio, A., Schnölzer, M., Sinha, P., and Federici, G. (2005) A proteomic investigation into etoposide chemo-resistance of neuroblastoma cell lines. *Proteomics* **5,** 796–804
53. Kanakkanthara, A., Rawson, P., Northcote, P. T., and Miller, J. H. (2012) Acquired resistance to Peloruside A and laulimalide is associated with down-regulation of vimentin in human ovarian carcinoma cells. *Pharm. Res.* **29,** 3022–3032
54. Arnesano, F., and Natile, G. (2009) Mechanistic insight into the cellular uptake and processing of cisplatin 30 years after its approval by FDA. *Coordin. Chem. Rev.* **253,** 2070–2081
55. Shen, D., Su, A., Liang, X., Pai-Panandiker, A., and Gottesman, M. (2004) Reduced expression of small GTPases and hypermethylation of the folate binding protein gene in cisplatin-resistant cells. *Br. J. Cancer* **91,** 270–276
56. Schwartz, S. L., Cao, C., Pylypenko, O., Rak, A., and Wandinger-Ness, A. (2007) Rab GTPases at a glance. *J. Cell Sci.* **120,** 3905–3910